



HAL
open science

Synchronous machine parameter identification by various excitation signals

Mourad Hasni, Omar Touhami, Rachid Ibtouen, Maurice Fadel, Stéphane Caux

► **To cite this version:**

Mourad Hasni, Omar Touhami, Rachid Ibtouen, Maurice Fadel, Stéphane Caux. Synchronous machine parameter identification by various excitation signals. *Electrical Engineering*, 2008, 90 (3), pp.219-228. 10.1007/s00202-007-0069-z . hal-03574315

HAL Id: hal-03574315

<https://ut3-toulouseinp.hal.science/hal-03574315>

Submitted on 15 Feb 2022

HAL is a multi-disciplinary open access archive for the deposit and dissemination of scientific research documents, whether they are published or not. The documents may come from teaching and research institutions in France or abroad, or from public or private research centers.

L'archive ouverte pluridisciplinaire **HAL**, est destinée au dépôt et à la diffusion de documents scientifiques de niveau recherche, publiés ou non, émanant des établissements d'enseignement et de recherche français ou étrangers, des laboratoires publics ou privés.

Synchronous machine parameter identification by various excitation signals

M. Hasni · O. Touhami · R. Ibtouen · M. Fadel · S. Caux

Abstract This paper presents the results of a time-domain identification procedure to estimate the linear parameters of a salient-pole synchronous machine at standstill. In this study, several input signals are used to identify the model structure and parameters of a salient-pole synchronous machine. The procedure consists to define, to conduct the standstill tests and also to identify the model structure. The signals used for identification are the different excitation voltages at standstill and the flowing current in different windings. We identify the parameters of operational impedances, in other words the reactances and time constants. The tests were carried out on synchronous machine of 1.5 kVA/380 V/1500 rpm.

Keywords Synchronous machine · Parameter identification · Standstill tests · (PRBS pseudo random binary sequences) voltages · PWM voltages and DC decay

List of symbols

p Laplace's operator
 ω, ω_0 angular speed
 ψ flux linkage
 X_f field leakage reactance
 X_d, X_q d - and q -axis synchronous reactances
 X_{md}, X_{mq} d - and q -axis magnetizing reactances

X_{Q1}, X_{Q2} q -axis damper leakage reactance
 r_{Q1}, r_{Q2} q -axis damper resistances
 $Y_{d,q}(p)$ d - and q -axis operational admittances
 T'_d, T'_{d0} d -axis transient open circuit and short-circuit time constant
 T'_q, T'_{q0} q -axis transient open circuit and short-circuit time constant
 T''_d, T''_{d0} d -axis subtransient open circuit and short-circuit time constant
 T''_q, T''_{q0} q -axis subtransient open circuit and short-circuit time constant
 r_a, r_f armature and field resistances
 V_d, V_q d - and q -axis stator voltages
 i_d, i_q d - and q -axis stator currents
 V_f, i_f d -axis field voltage and current

1 Introduction

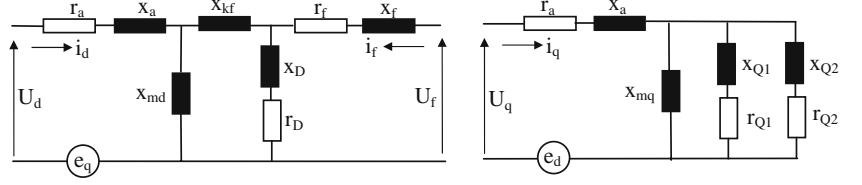
Many methods for determination synchronous machine parameters have been suggested. Among them are neural networks, finite elements, online and off-line statistical methods, frequency response, load rejection and others [1–5]. The identification of synchronous machine parameters has been and still is an important subject of many publications. Various measurement techniques, identification procedures and models structures are developed to obtain models with accurate prediction for the transient behaviour of generators.

Many approaches are suggested in several paper, dealing with synchronous machine modelling and parameter estimation. Among these methods are standstill frequency response data, standstill time response data, and rotating time domain response data [1–6]. The standstill modelling approach is one which has received great attention due to its relatively simple testing method where the d and q axis are decoupled.

M. Hasni · O. Touhami (✉) · R. Ibtouen
Electrical Engineering Department,
National Polytechnic School of Algiers, 10, av. Pasteur,
El Harrach, BP 182, Algiers 16200, Algeria
e-mail: omar.touhami@enp.edu.dz

M. Fadel · S. Caux
Laboratoire Plasma et Conversion d'Énergie,
Unité mixte CNRS-INP Toulouse,
2, rue Camichelle, BP 7122,
31071 Toulouse Cedex 7, France

Fig. 1 Standard d - q axis circuit models



In this context, we present off-line parameter identification for the synchronous machine. In this study the armature of synchronous machine is successively fed at standstill by DC-Chopper, (PRBS pseudo random binary sequences) voltages, PWM voltages and DC decay.

A systematic identification procedure presented in Sect. 3 is used to estimate the machine parameters and equivalent circuit models directly from the time response data. [7–9]

In the time-domain analysis, there is a non-linear problem difficulty to solve. Our approach is based on Levenberg–Marquardt algorithm.

In this present research work system identification model concepts and standstill time data are used to identify the parameters of synchronous machine with the following specifications: 1.5 kVA, 380 V, and 1500 rpm.

2 Synchronous machine modelling

For synchronous machine studies, two-axis equivalent circuits with two or three damping windings are usually assumed at the proper structures [6]. Using the Park's d and q -axis reference frame, the synchronous machine is supposed to be modelled with one damper winding for the d -axis and two windings for the q -axis (2×2 model) as shown in Fig. 1 [9–12].

2.1 Voltage equations

$$V_d(p) = r_a i_d(p) + p\psi_d(p) - \omega_r \psi_q(p) \quad (1.a)$$

$$V_q(p) = r_a i_q(p) + p\psi_q(p) + \omega_r \psi_d(p) \quad (1.b)$$

$$V_f(p) = r_f i_f(p) + p\psi_f(p) \quad (1.c)$$

$$0 = r_D i_D(p) + p\psi_D(p) \quad (1.d)$$

$$0 = r_Q i_Q(p) + p\psi_Q(p) \quad (1.e)$$

While eliminating $\psi_f, i_f, \psi_D, i_D, \psi_Q, i_Q$ we obtains the following equations:

$$V_d(p) = r_a i_d(p) + p\psi_d(p) - \omega_r \psi_q(p) \quad (2.a)$$

$$V_q(p) = r_a i_q(p) + p\psi_q(p) + \omega_r \psi_d(p) \quad (2.b)$$

$$\psi_d(p) = X_d(p) i_d(p) + G(p) V_f(p) \quad (2.c)$$

$$\psi_q(p) = X_q(p) i_q(p) \quad (2.d)$$

This writing form of the machine equations has the advantage of being independent of number of damper windings

considered on each axis. In fact, it is the order of the functions $X_d(p)$, $X_q(p)$ and $G(p)$, which depend on the number of dampers.

2.2 Reduced model order

In theory, we can represent a synchronous machine by an unlimited stator and rotor circuits. However, the experience show, in modelling and identification there is seven models structures which can be used. The complex model is the 3×3 model which have a field winding, two damper windings on the direct axis, and three on the quadrature axis.

The more common representation is the one deduced from the second order characteristic equation which describes the 2×2 model [8–10].

Damper circuits, especially those in the quadrature axis provide much of the damper torque. This particularity is important in studies of small signal stability, where conditions are examined about some operating point [10]. The second order direct axis models includes a differential leakage reactance. In certain situations for second order models, the identity of the transients field winding. Alternatively, the field circuit topology can alter by the presence of an excitation system, with its associated non-linear features.

For machine at standstill, the rotor speed is zero ($\omega = 0$) and using the p Laplace's operator, the voltage equations are:

– For the d -axis

$$V_d = \left[r_a + \frac{p}{\omega_0} X_d(p) \right] i_d + pG(p)v_f \quad (3.a)$$

$$V_f = \left[r_f + \frac{p}{\omega_0} X_f(p) \right] i_f + \frac{p}{\omega_0} X_{md} i_d \quad (3.b)$$

– For the q -axis

$$V_q = \left[r_a + \frac{p}{\omega_0} X_q(p) \right] i_q \quad (3.c)$$

With the operational reactances are:

$$X_{d,q,f}(p) = X_{d,q,f} \frac{(1 + pT'_{d,q,f}) (1 + pT''_{d,q,f})}{(1 + pT'_{d0,q0,f0}) (1 + pT''_{d0,q0,f0})} \quad (4.a)$$

The operational function $G(p)$ is:

$$G(p) = \frac{X_{md}}{r_f} \frac{1}{1 + pT'_{d0}}. \quad (4.b)$$

From these equations it follows that only the three functions $X_d(p)$, $X_q(p)$ and $G(p)$ are necessary to identify a synchronous machine. In the original theory, the quadrature axis has no transient quantities. However, the DC measurements at standstill recommended by IEC, and also the short-circuit tests in the quadrature axis show that the real machine also has transient values $X'_q(p)$, T'_q in addition to the sub transient values $X''_q(p)$, T''_q .

In this study, voltage is the input signal and current is the output signal. Therefore, the transfer functions are in admittances form.

The reduced operational admittances of d -axis and q -axis are deduced from the input–output signals

$$Y_{d,q}(p) = \frac{i_{d,q}(p)}{V_{d,q}(p)} \quad (5.a)$$

In other words:

$$Y_{d,q}(p) = \frac{1 + p(T'_{d0,q0} + T''_{d0,q0}) + p^2 T'_{d0,q0} T''_{d0,q0}}{r_a + A \cdot p + B \cdot p^2 + C \cdot p^3} \quad (5.b)$$

With:

$$A = r_a \left((T'_{d0,q0} + T''_{d0,q0}) + \frac{x_{d,q}}{\omega_0} \right),$$

$$B = \left(r_a T'_{d0,q0} T''_{d0,q0} + \frac{x_{d,q}}{\omega_0} (T'_{d,q} + T''_{d,q}) \right), \quad C = \frac{x_d}{\omega_0} T'_{d,q} T''_{d,q}$$

The reduced operational admittances take the following forms

$$H_{d,q}(p) = \frac{b_0 + b_1 \cdot p + b_2 \cdot p^2}{1 + a_1 \cdot p + a_2 \cdot p^2 + a_3 \cdot p^3} \quad (6.a)$$

The synchronous machine parameters are identified by:

$$b_0 = \frac{1}{r_a} \quad (6.b)$$

$$b_1 = \frac{T'_{d0,q0} + T''_{d0,q0}}{r_a} \quad (6.c)$$

$$b_2 = \frac{T'_{d0,q0} T''_{d0,q0}}{r_a} \quad (6.d)$$

$$a_1 = T'_{d0,q0} + T''_{d0,q0} + \frac{x_{d,q}}{\omega_0 r_a} \quad (6.e)$$

$$a_2 = \frac{x_{d,q}}{\omega_0 r_a} (T'_{d,q} + T''_{d,q}) + T'_{d0,q0} T''_{d0,q0} \quad (6.f)$$

$$a_3 = \frac{x_{d,q}}{\omega_0 r_a} T'_{d,q} T''_{d,q} \quad (6.g)$$

Equations (6.a–6.g) show that to determine the various parameters and time-constants of the machine, we have to calculate the constants values a_1 , a_2 , a_3 , b_0 , b_1 and b_2 by using the non-linear programming method. For this reason

we have used a program, which makes it possible to compute from the input–output signals for each axis (see Figs. (3, 4, 5, 6)), the parameters quoted above. The model structure selected, which means that the form of the transfer function is known. The numerator order and the denominator one are, respectively: Num = 2 and Den = 3.

The objective of our identification task is to compare the simulated model response and the actual response by minimizing the error between them. For minimizing this error, a good optimisation technique is needed. For that we used a quadratic criterion to quantify the difference between the process and the model. Our approach is based on Levenberg–Marquardt algorithm.

2.3 Levenberg–Marquardt's algorithm

The Levenberg–Marquardt algorithm [13,14] is a general non-linear downhill minimisation algorithm for the case when derivatives of the objective function are known. It dynamically mixes Gauss–Newton and gradient-descent iterations. The unknown parameters be represented by the vector x , and let noisy measurements of x be made:

$$z(j) = h(j; x) + w(j), \quad j = 1, \dots, k \quad (7.a)$$

Where $h(j)$ is a measurement function and $w(j)$ is zero-mean noise with covariance $N(j)$. Since, we are describing an iterative minimization algorithm, we shall assume that we have an estimate \hat{x}^- of x . A new estimate \hat{x} maximizes

$$\chi^2(\hat{x}) = \sum_{j=1}^k (z(j) - h(j; \hat{x}))^T N(j)^{-1} (z(j) - h(j; \hat{x})) \quad (7.b)$$

We form a quadratic approximation to $\chi^2(\cdot)$ around \hat{x}^- , and minimize this approximation to $\chi^2(\cdot)$ to obtain a new estimate \hat{x}^+ . In general we can write such a quadratic approximation as

$$\chi^2(x) \approx \alpha - 2a^T (x - \hat{x}^-) + (x - \hat{x}^-)^T A (x - \hat{x}^-)$$

for scalar α , vector a and matrix A . Afterwards differentiating we obtain

$$\frac{\partial \chi^2}{\partial x} = -2a + 2A(x - \hat{x}^-).$$

$$\frac{\partial^2 \chi^2}{\partial x^2} = 2A,$$

At the minimum point \hat{x} we have $\frac{\partial \chi^2}{\partial x} = 0$ which means that

$$A(\hat{x}^+ - \hat{x}^-) = a. \quad (7.c)$$

Thus we need to obtain a and A to compute the update. We now consider the form of $\chi^2(\cdot)$ in (7.b) Writing the Jacobian of $h(j, x)$ as $H(j) = \frac{\partial h(j)}{\partial x}$.

We have

$$\frac{\partial \chi^2}{\partial x} = -2 \sum_{j=1}^k H(j)^T N(j)^{-1} (z(j) - h(j; x)), \quad (7.d)$$

$$\begin{aligned} \frac{\partial^2 \chi^2}{\partial x^2} &= 2 \sum_{j=1}^k H(j)^T N(j)^{-1} H(j) \\ &\quad - 2 \sum_{j=1}^k \left(\frac{\partial H(j)}{\partial x} \right)^T N(j)^{-1} (z(j) - h(j; x)) \\ &\approx 2 \sum_{j=1}^k H(j)^T N(j)^{-1} H(j), \end{aligned} \quad (7.e)$$

In the last formula for $\partial^2 \chi^2 / \partial x^2$, the terms involving the second derivatives of $h(j)$ have been omitted. This is done because these terms are generally much smaller and can in practice be omitted.

Now we solve the above equations for a and A given the values of function $h(j)$ and the Jacobian $H(j)$ evaluated at the previous estimate \hat{x}^- . We have immediately

$$A = \sum_{j=1}^k H(j)^T N(j)^{-1} H(j)$$

We now write the innovation vectors $v(j)$ as

$$v(j) = z(j) - h(j; \hat{x}^-)$$

Then we have

$$a = \sum_{j=1}^k H(j)^T N(j)^{-1} v(j) \quad (7.f)$$

Combining Eqs. (7.c) and (7.f) we obtain the linear system

$$A(\hat{x}^+ - \hat{x}^-) = a = \sum_{j=1}^k H(j)^T N(j)^{-1} v(j) \quad (7.g)$$

To be solved for the adjustment $\hat{x}^+ - \hat{x}^-$. The covariance of the state is $P = A^{-1}$

The update (7.g) may be repeated, substituting the new \hat{x}^+ as \hat{x}^- , and improving the estimate until convergence is achieved according to some criterion. Levenberg–Marquardt modifies this updating procedure by adding a value λ to the diagonal elements of the linear system matrix before inverting it to obtain the update. λ is reduced if the last iteration gave an improved estimate, i.e. if χ^2 was reduced, and increased if J increased, in which case the estimate of x is reset to the estimate before the last iteration. It is this that allows the algorithm to smoothly switch between Gauss–Newton (small λ) and gradient descent (large λ). The full algorithm is as follow:

1. Start with an estimate \hat{x}^- of x . Initialize λ to some starting value (e.g. 0.001)

2. Compute the update estimate \hat{x}^+ by solving the linear system (7.g) for the adjustment, having first added λ to each diagonal element of A
3. Compute the least-squares residuals $\chi^2(\hat{x}^-)$ and $\chi^2(\hat{x}^+)$ from (7.b)
 - (a) - If $\chi^2(\hat{x}^+) < \chi^2(\hat{x}^-)$, reduce λ by a specified factor (say 10), set \hat{x}^- to \hat{x}^+ , and return to step 2
 - (b) - Otherwise, the update failed to reduce the residual, so increase λ by a factor (say 10), forget the updated \hat{x}^+ and return to step 2

The algorithm continues until some pre-specified termination criterion has been met, such as a small change to the state vector, or a limit on the number of iterations.

3 Identification of the synchronous machine parameters

In this section, the practical aspects of measurements are described and machine conditions for standstill tests are also given [15–17]. The tests are described in IEC34–4A and ANSI-IEEE Std.115A publications [4,5]. It is very easy to perform in practice. PRBS voltages, PWM voltages and DC voltages are applied to two terminals of the three-phase stator windings at standstill. The alignment of the rotor can be accomplished with shorted excitation winding; a sinewave voltage is applied between two phases of the stator. The duration of the voltage application should be limited to avoid serious overheating of solid parts. The rotor is slowly rotated to find the angular positions corresponding to the maximum value of the excitation current that gives the direct axis and zero value of the excitation winding current that corresponds to the quadrature axis. This procedure is used by the authors [4,8,9]. Figure 2 shows the experimental procedure of identification.

The machine is not saturated during standstill tests; in fact, the flux densities are below those on the more linear part of the permeability characteristic that is commonly referred to as “unsaturated”. The determination of quantities referred to the unsaturated state of the machine must be done from tests with supply voltage (1–2%) of the nominal values.

3.1 Experimental procedure

The two principal characteristic parameters, which relate to the definitions listed, are:

- $Z_d(p)$: the direct-axis operational impedance equal to $r_a + p \cdot l_d(p)$, where r_a is the DC armature resistance per phase
- $Z_q(p)$: the quadrature-axis operational impedance equal to $r_a + p \cdot l_q(p)$.

Fig. 2 Experimental procedure of identification

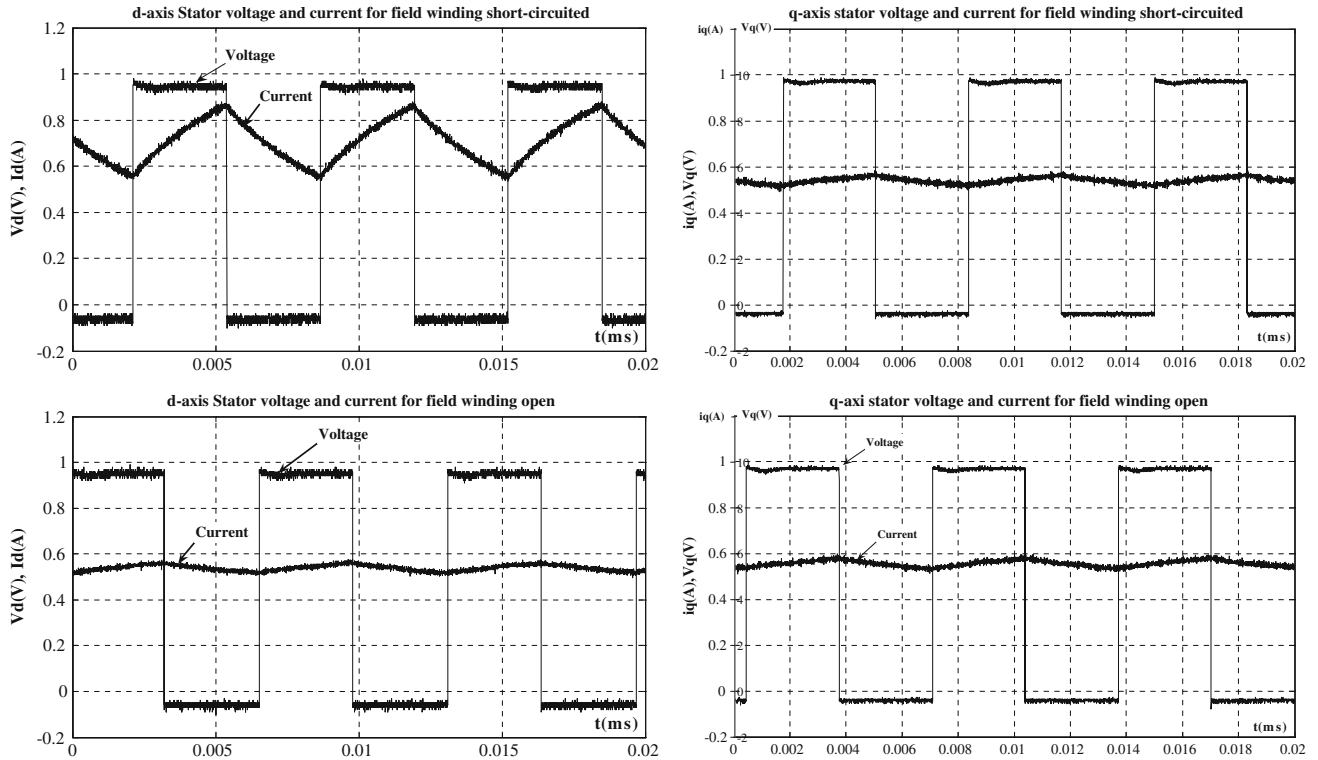
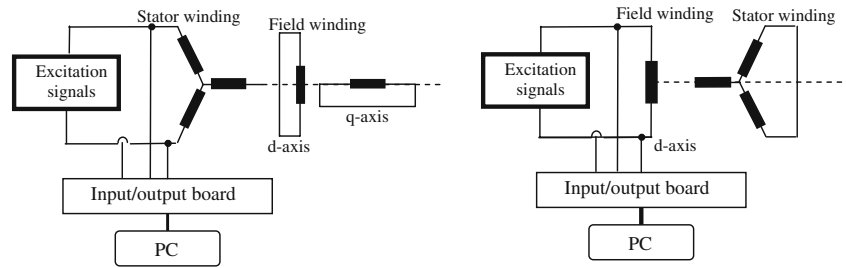


Fig. 3 Windings excited by a DC-Chopper

The above two quantities are the stator driving point impedances. An alternative method of measuring this parameter is presented as follows:

$$G(p) = \frac{I_{fd}(p)}{pI_d(p)} \quad \text{for } E_{fd} = 0 \quad (8)$$

Short-circuited field winding ($V_f = 0$), the d - and q -axis operational admittances are given:

$$Y_{d,q}(p) = \frac{i_{d,q}(p)}{V_{d,q}(p)} \quad \text{for } V_f = 0 \quad (9)$$

Short-circuited d -axis stator winding ($V_d = 0$), the field winding parameters can be obtained by:

$$Y_f(p) = \frac{i_f(p)}{V_f(p)} \quad \text{for } V_d = 0 \quad (10)$$

Some experimental input–output data such as stator voltages and currents for open and short-circuited field winding, respectively are presented in: Fig. 3 (the windings are excited by a DC-Chopper); Fig. 4 (the windings are excited by PRBS voltages); Fig. 5 (the windings are excited by a DC voltage); Fig. 6 (the windings are excited by a PWM voltages).

3.2 Experimental results

Table 1 presents the parameter values of a synchronous machine from tests using in this study.

The time domain approach offers a method, which can yield useful models, particularly if the data are correctly treated. Taking into account the difficulties associated to the classical test analysis, the identification of synchronous machine is more and more oriented to the static tests.

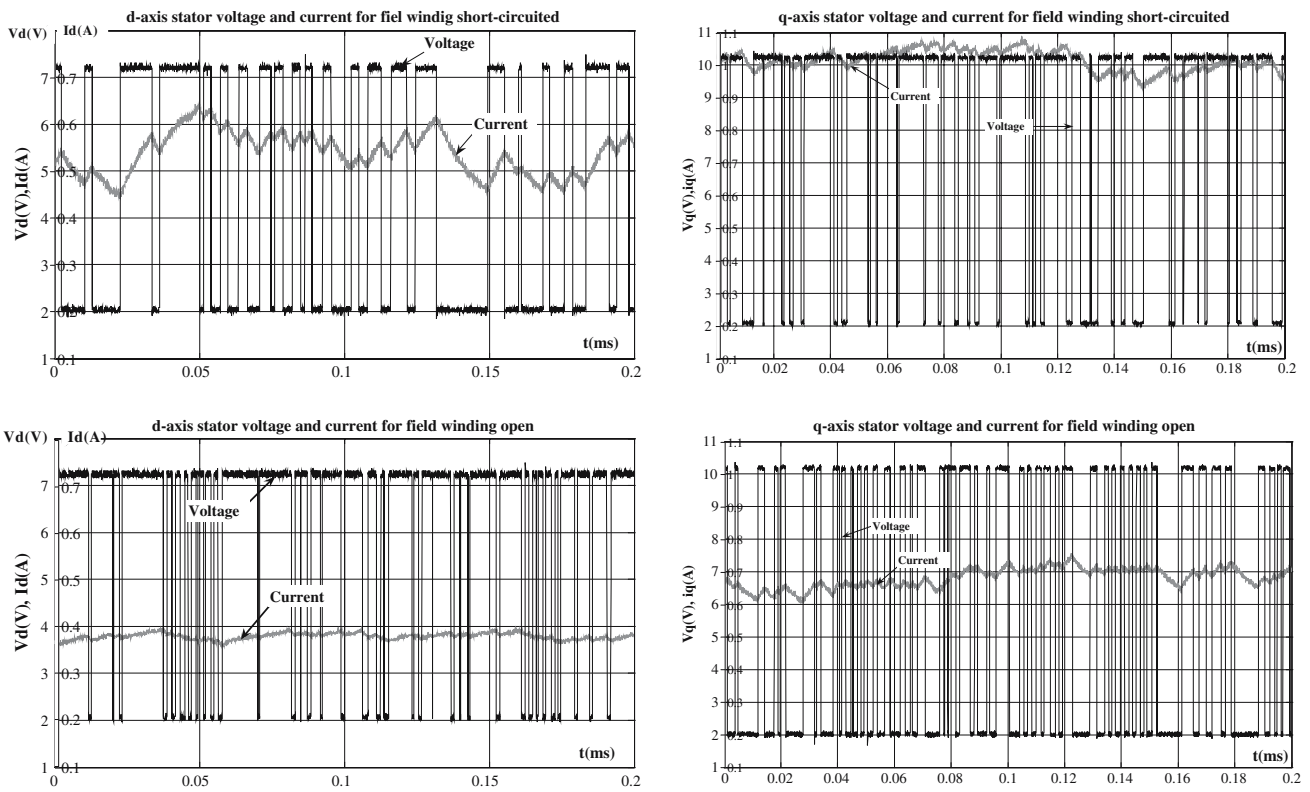


Fig. 4 Windings excited by PRBS voltages

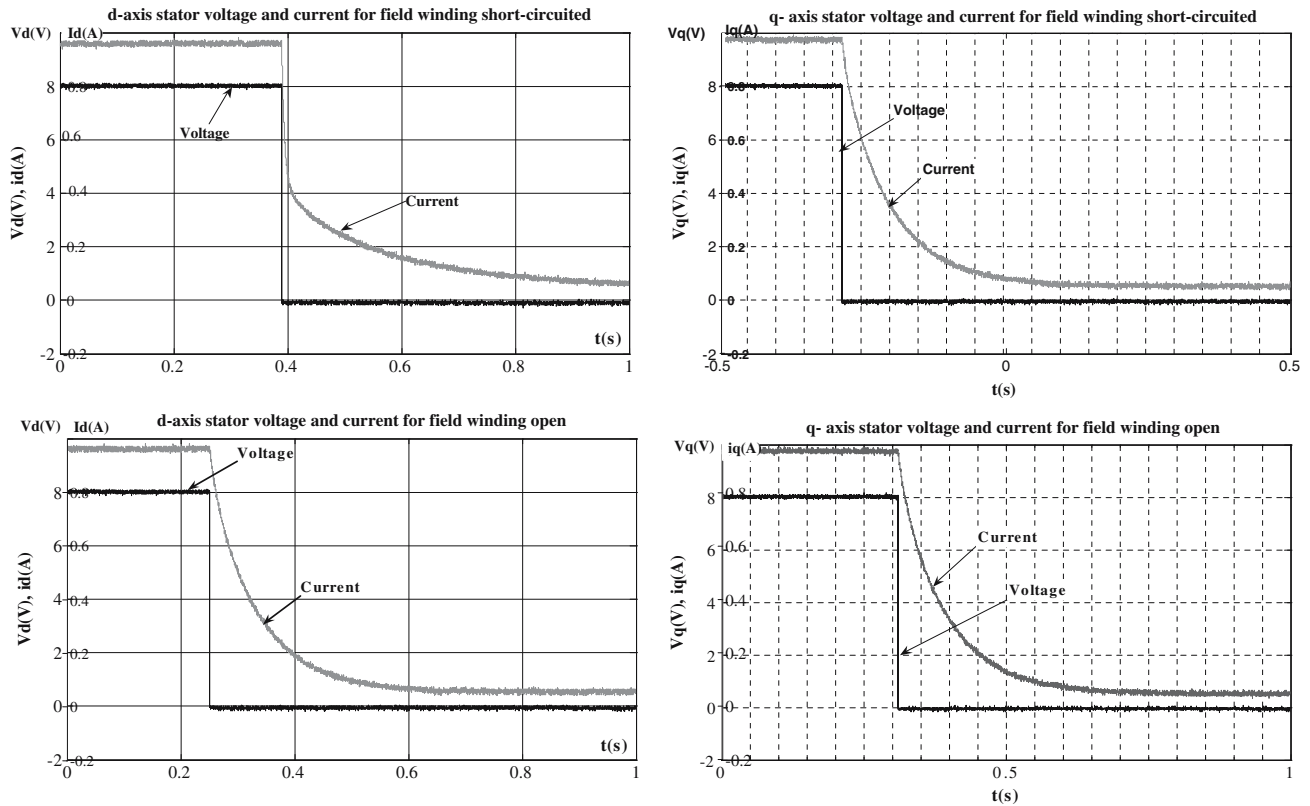


Fig. 5 Windings excited by a DC voltage

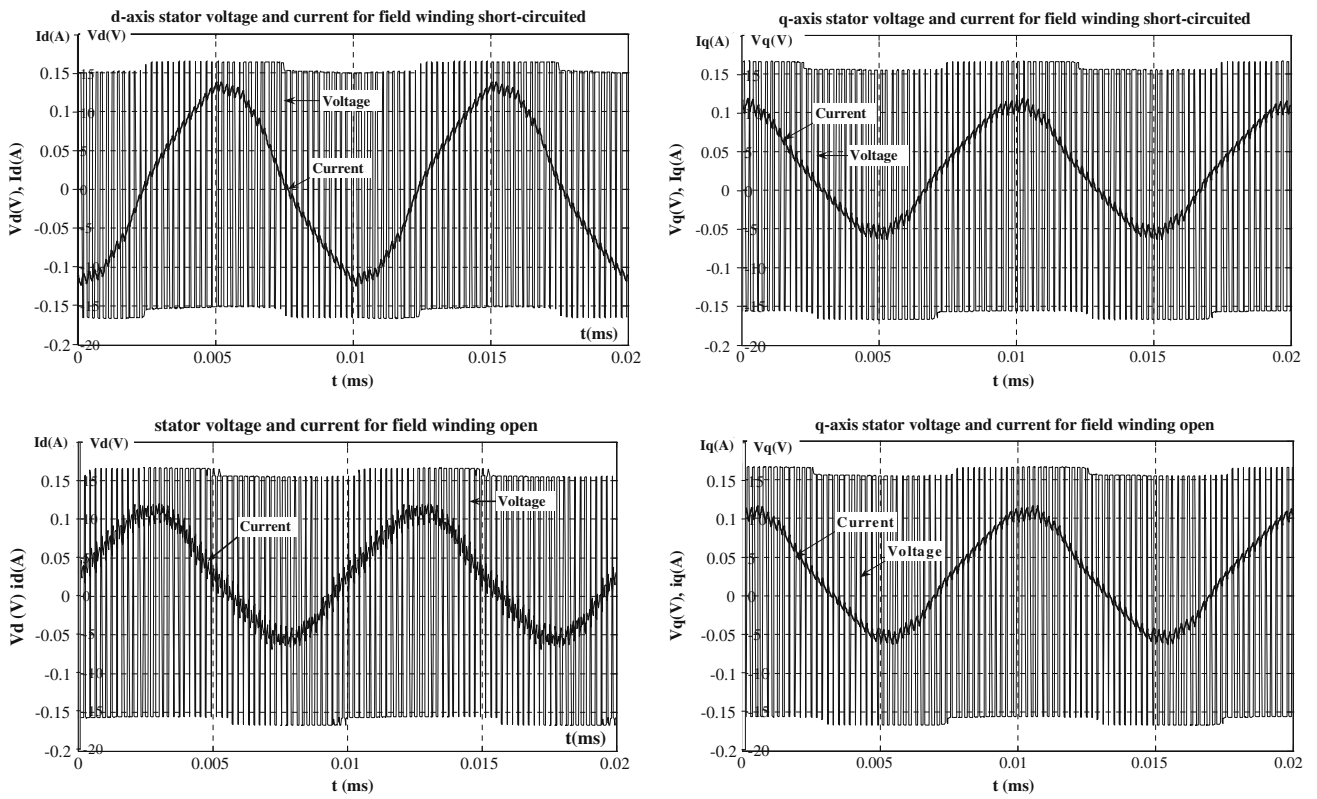


Fig. 6 Windings excited by PWM voltages

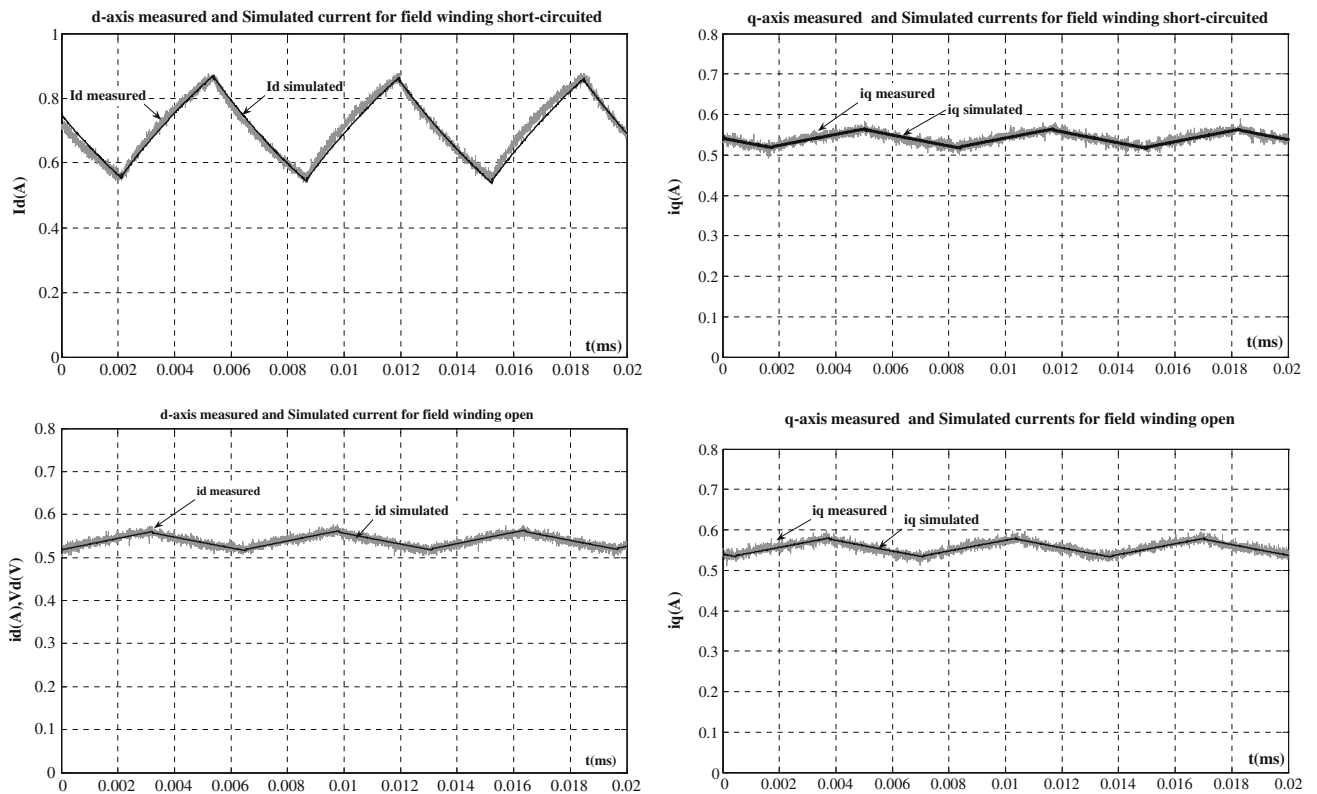


Fig. 7 Comparison between real data output and simulated data output, armature current for field winding open and short circuited (DC-chopper voltages), respectively

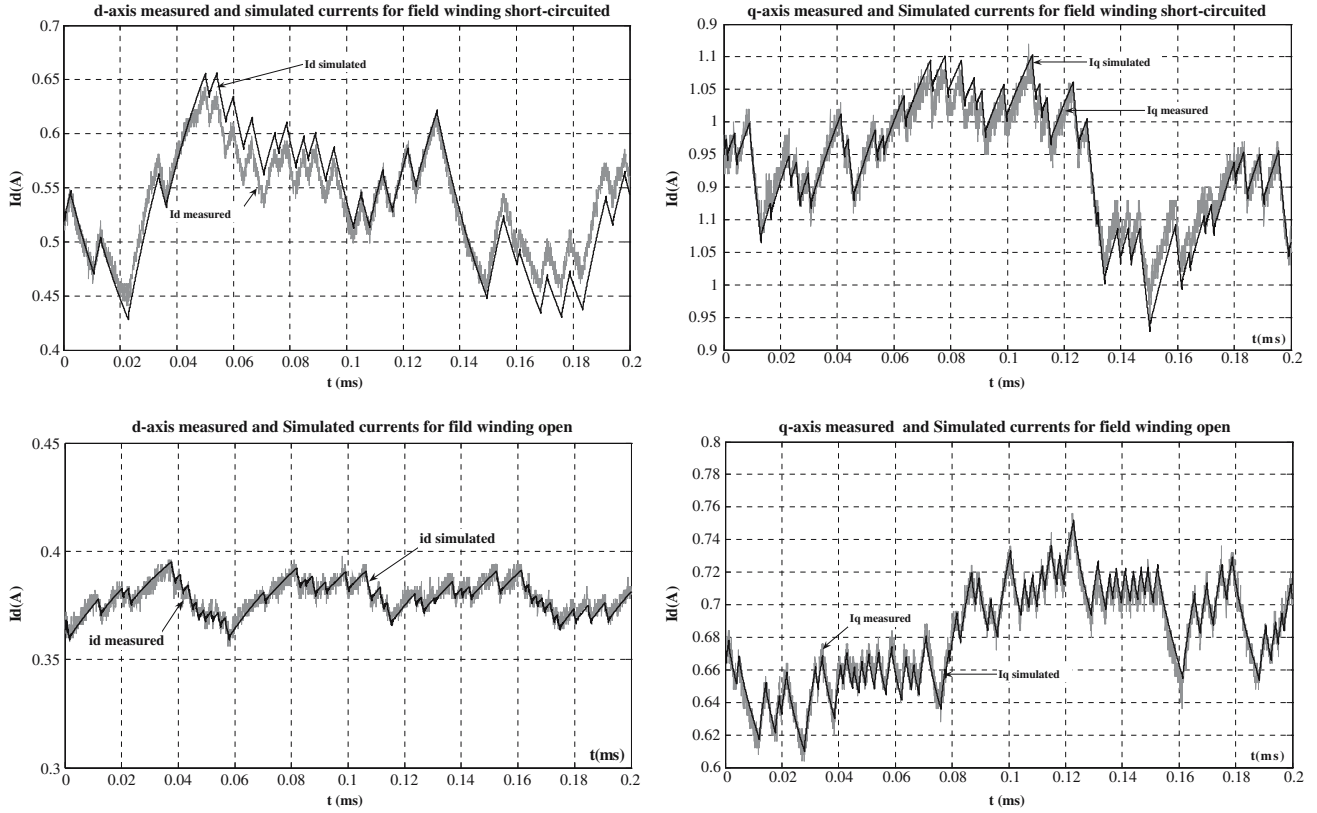


Fig. 8 Comparison between real data output and simulated data output, armature current for field winding open and short circuited (PRBS voltages), respectively

Table 1 Synchronous machine parameter values identified by four excitation signals

Parameters	DC-chopper voltages	PRBS voltages	DC decay	PWM voltages
R_a (p.u)	0.149	0.149	0.149	0.149
R_f (p.u)	4.95	4.95	4.95	4.95
T'_d (s)	0.1856	0.1675	0.1840	0.2045
T''_d (s)	0.0490	0.0526	—	0.0471
T'_{d0} (s)	1.0907	0.9189	1.1346	1.1943
T''_{d0} (s)	0.4350	0.4785	—	0.5060
T'_q (s)	0.1476	0.1284	0.1509	0.1782
T''_q (s)	0.0461	0.0361	—	0.0432
T'_{q0} (s)	0.9022	0.7849	1.0279	1.0360
T''_{q0} (s)	0.4631	0.3829	—	0.4348
X_d (p.u)	2.0667	1.9980	2.0515	1.9314
X'_d (p.u)	0.3516	0.3459	0.3758	0.3857
X_q (p.u)	1.3378	1.5639	1.3880	1.6328
X'_q (p.u)	0.2089	0.1904	0.2413	0.2158
X''_d (p.u)	0.0396	0.0345	—	0.0343
X''_q (p.u)	0.0218	0.0198	—	0.0209

Nevertheless, the choice of supply signals is very important as the choice of model.

The proposed model, the quality and the experimental data used to identify the model parameters and the robustness of the estimation technique affects the fidelity of synchronous machine models. It is well known that the synchronous machine has a highly complex structure. However, under practical consideration, such complexity has been redefined and reduced following the intended application [8].

3.3 Model validation

The identified d - q axis models are verified by comparing their simulated d - q axis stator currents responses against the measured standstill response, for that we present in Fig. 7, 8, 9, 10 simulation results for chosen signals among those presented previously. The measured and simulated responses to off-line excitation disturbances comparison show that the machine linear parameters are accurately estimated to represent the machine at standstill conditions.

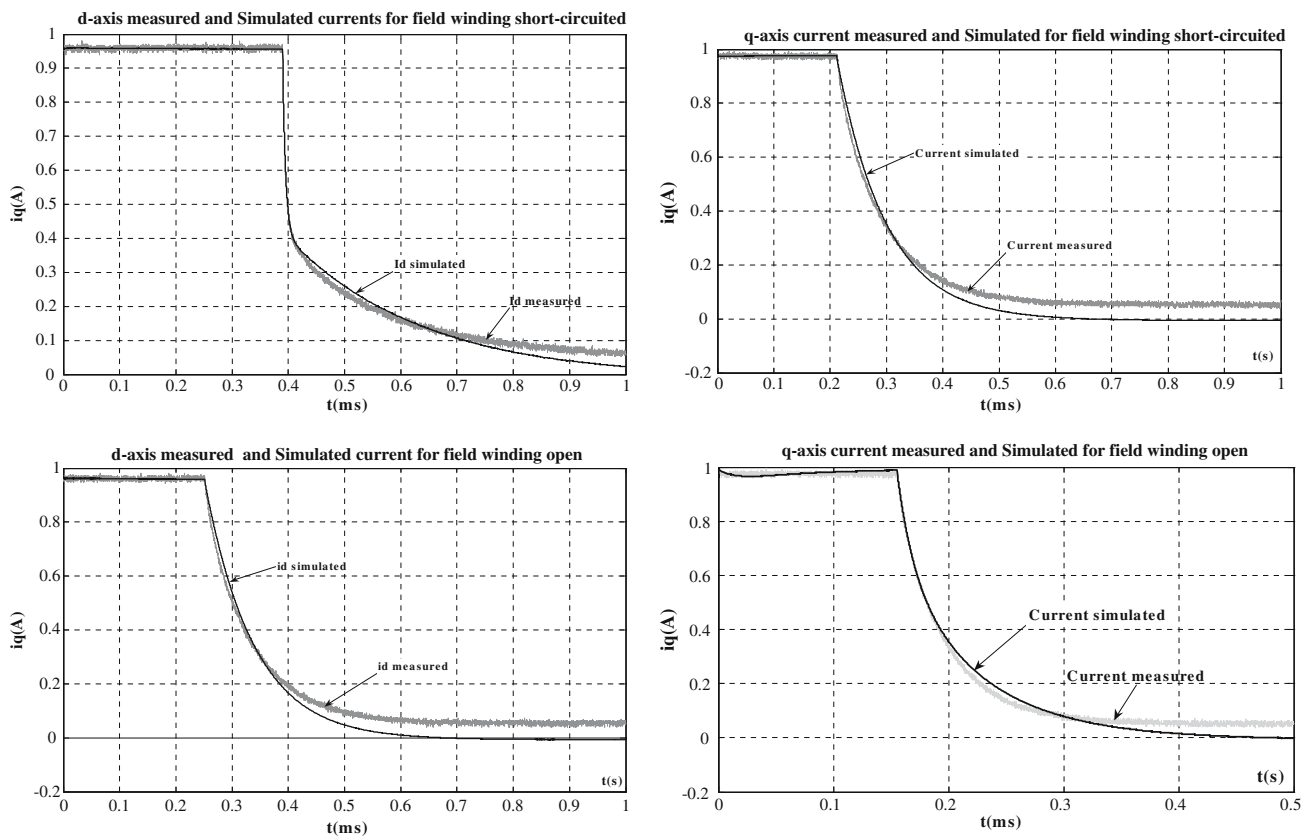


Fig. 9 Comparison between real data output and simulated data output, armature current for field winding open and short circuited (DC decay), respectively

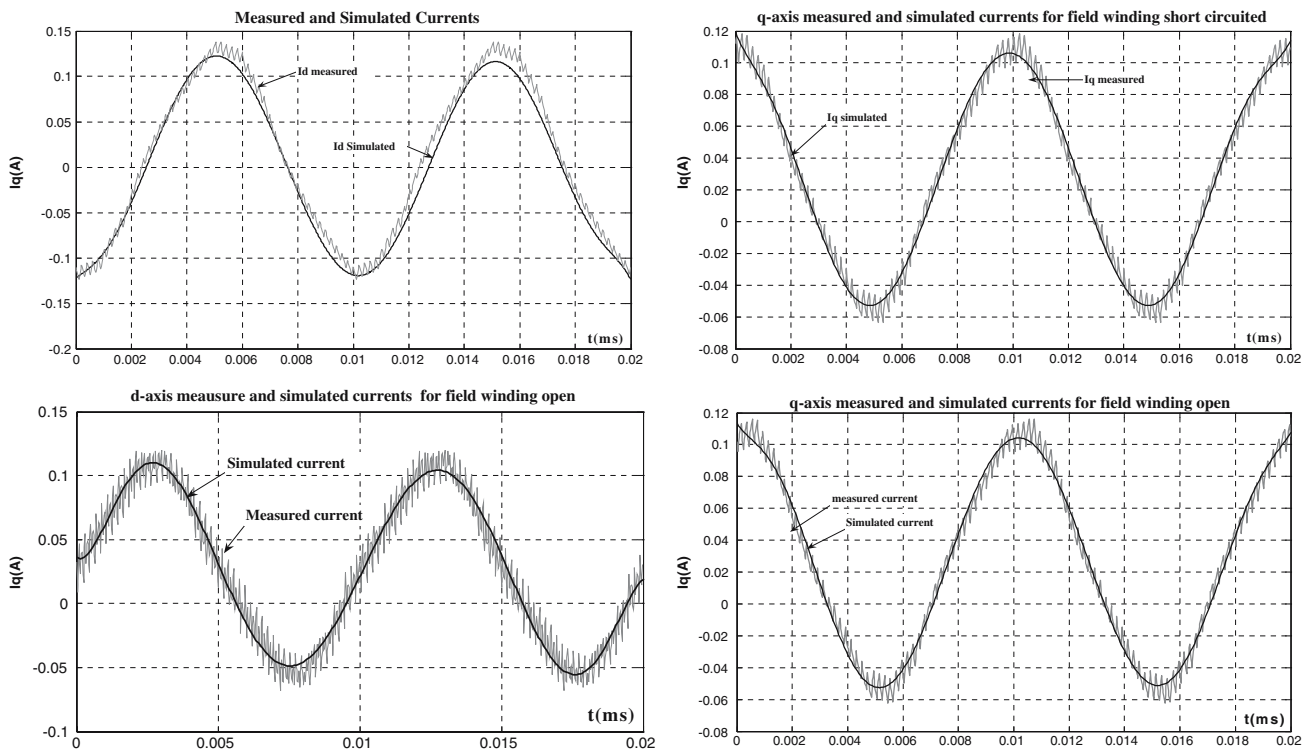


Fig. 10 Comparison between real data output and simulated data output, armature current for field winding open and short circuited (PWM voltages), respectively

4 Conclusion

This paper presents a step-by-step procedure to identify the parameter values of the d - q axis synchronous machine models using the standstill time-domain data analysis.

A three-phase salient-pole laboratory machine rated 1.5 kVA and 380 V is tested at standstill and its parameters are estimated. Both the transfer function model and the equivalent circuit model parameters are identified using the Levenberg–Marquardt algorithm.

The standstill test concept is preferred because there is no interaction between the direct and the quadrature axis, and it can be concluded that the parameter identification for both axis may be carried out separately. This tests method had been used successfully on our synchronous machine at standstill and gave all the Parks model parameters. Among the advantages claimed for the time-domain approach at standstill is that the tests are safe and relatively inexpensive.

It should be noted that the various signals used made it possible to determine all the parameters of the equivalent circuits, except for the dc decay test which does not enable us to determine the parameters varying very fast. The identified parameters are in agreement for different tests signals. Furthermore, information's about the quadrature axis, as well as the direct axis of the machine are obtained. We notice that, it can be possible to realise a parameter estimation of large power synchronous machine or turbo generators. The validation of the estimated synchronous machine model parameters is performed by direct comparisons between the measured and simulated standstill time domain responses. The results show that the machine linear parameters are accurately estimated to represent the machine standstill condition.

Acknowledgment The authors of Laboratories LRE and LAPLACE, respectively of the ENP Algiers and the ENSEIHT Toulouse make a point of announcing that this work enters within the framework of an international project of co-operation, Agreement—CMEP Tassili, under the code 05 MDU 662.

References

1. Bortoni EC, Jardini JA (2004) A standstill frequency response method for large salient pole synchronous machines. *IEEE Trans on E.C* 19(4):687–691
2. Henschel S, Dommel HW (1999) Noniterative synchronous machine parameter identification from frequency response tests. *IEEE Trans Power Syst* 14:553–560
3. IEEE Task force on definition (PL Dandeno Chairman) (1986) Current usage and suggested practices in power stability simulations for synchronous machines. *IEEE Trans On E.C* EC-1(1) pp 77–93
4. IEC (1985) Recommendations for rotating electrical machinery. Part. 4 'methods for determining synchronous machine quantities' IEC pp 34–4A
5. IEEE Guide (1995) Test procedures for synchronous machines, IEEE Std. 115A
6. Guesbaoui H, Iung C, Touhami O (1995) Towards a real time Parameter identification methodology for electrical machines. *IEEE-PES/KTH Stockholm Power Tech Conf* pp 91–96
7. Horning S, Keyhani A, Kamwa I (1997) On-line Evaluation of a round rotor synchronous machine parameter set estimation from standstill time-domain data. *IEEE Trans on E.C* 12(4):289–296
8. Kamwa I, Viarouge P, Dickinson EJ (1990) Experimental modeling of a synchronous machine-chopper system standstill normal operating records. *IMACS-TC1* 1:247–253
9. Hasni M, Touhami O, Ibtouen R, Fadel M (2006) Modelling and identification of a synchronous machine by using singular perturbations. *IREE*, July–August 2006, pp 418–425
10. Touhami O, Guesbaoui H, Iung C (1994) Synchronous machine parameter identification by a multi-time scale technique. *IEEE Trans On Ind. Appl* IA-30(5):1600–1608
11. Tumageanian A, Keyhani A (1995) Identification of synchronous machine linear parameters from standstill step voltage input data. *IEEE Trans on E.C* 10(2):232–239
12. Nele D, Pintelon R, Lataire P (2003) Estimation of a global synchronous machine model using a multiple input multiple output estimators. *IEEE Trans. On E.C* 18(1):11–16
13. Bjorck A (1996) Numerical methods for least square problems. *SIAM Press*, Philadelphia
14. Marquardt DW (1983) An algorithm for least-squares estimation of nonlinear parameters. *J Soc Ind Appl Math* 11:431–441
15. Graza V, Biriescu M, Liuba Gh, Cretu V (2001) Experimental determination of synchronous machines reactances from DC decay at standstill. *IEEE Instrumentation and measurement technology conference*, Budapest, Hungary, pp 1954–1957, May 2001
16. Verbeeck J, Pintelon R, Lataire P (1999) Identification of synchronous machine parameters using a multiple input output approach. *IEEE Trans on E.C* 14(4):909–916
17. Bora Karayaka H, Keyhani A, Agrawal BI, Selin DA, Heydt GT (2000) Identification of armature, field, and saturated parameters of large steam turbine-generator from operating data. *IEEE Trans on E.C* 15(2):181–187